Differential patterning of cGMP in vascular smooth muscle cells revealed by single GFP-linked biosensors

Lydia W. M. Nausch, Jonathan Ledoux, Adrian D. Bonev, Mark T. Nelson, and Wolfgang R. Dostmann*

Department of Pharmacology, University of Vermont College of Medicine, Burlington, VT 05405

Communicated by Susan S. Taylor, University of California at San Diego, La Jolla, CA, November 7, 2007 (received for review September 20, 2007)

Here, we report the design of unprecedented, non-FRET based cGMP-biosensors, named FlincGs, to assess the dynamics of nitric oxide (NO) and atrial natriuretic peptide (ANP) induced synthesis of intracellular cGMP, $[cGMP]_i$. Regulatory fragments of PKG I α, PKG I β, and an N-terminal deletion mutant of PKG I α were fused to circular permutated EGFP to generate α-, β-, and δ-FlincG, with high dynamic ranges and apparent $K_{D,cGMP}$ values of 35 nM, 1.1 μM, and 170 nM, respectively. All indicators displayed significant selectivity for cGMP over cAMP, and 1.5- to 2.1-fold increases in fluorescence intensity at 510 nm when excited at 480 nm. Surprisingly, FlincGs displayed an additional excitation peak at 410 nm. δ-FlincG permitted ratiometric (480/410 nm) measurements, with a cGMP-specific 3.5-fold ratio change. In addition, δ-FlincG presented cGMP association and dissociation kinetics sufficiently fast to monitor rapid changes of $[cGMP]_i$ in intact cells. In unpassaged, adenoviral transfected vascular smooth muscle (VSM) cells, δ-FlincG had an $EC_{50,cGMP}$ of 150 nM, and revealed transient global cGMP elevations to sustained physiological NO ($EC_{50,DEA/NO}$ = 4 nM), and the decay phase depended on the activity of PDE-5. In contrast, ANP elicited sustained submembrane elevations in $[cGMP]_i$, which were converted to global cGMP elevations by inhibition of PDE-5 by sildenafil. These results indicate that FlincG is an innovative tool to elucidate the dynamics of a central biological signal, cGMP, and that NO and natriuretic peptides induce distinct cGMP patterning under the regulation of PDE-5, and therefore likely differentially engage cGMP targets.

fluorescent biosensors | natriuretic peptides | nitric oxide | confocal microscopy | cGMP-dependent protein kinase

Cyclic 3′,5′-guanosine monophosphate (cGMP) has profound effects on cell function through actions on cGMP-specific phosphodiesterases (PDEs) and cGMP-dependent protein kinases (PKGs), as well as through several types of cyclic nucleotide-activated ion channels (CNGs) (1–4). cGMP is synthesized by two distinct families of guanylyl cyclases: (*i*) the natriuretic peptide-specific, plasma membrane-associated guanylyl cyclases (pGC), and (*ii*) the nitric oxide (NO)-activated, cytosolic soluble guanylyl cyclases (sGC) (5–8). Intracellular cGMP levels are terminated through the hydrolyzing activities of cGMP-specific phosphodiesterases (1).

In recent years, several FRET-based cGMP indicators have been developed in an effort to monitor spatiotemporal dynamics of $[cGMP]_i$ (9–11). Particularly, Cygnet-type cGMP indicators have significantly advanced our understanding of cGMP dynamics in VSM and other cell types (9, 12–16). However, FRET-based cGMP indicators have limitations. They require a technically laborious dual emission detection system and generally show overall low cyan/yellow emission ratio changes in intact cells. Furthermore, at low, physiological NO-concentrations (<10 nM), FRET-based cGMP indicators are limited in their use to detect fluctuations in $[cGMP]_i$ (12). However, recent studies using purified cyclase, intact platelets and cerebellar cells have shown that sGC is activated at low-nanomolar NO concentrations (1–10 nM) (17, 18). FRET-based cGMP indicators are also limited in resolving possible compartmentalized intracellular cGMP signaling events using confocal microscopy. It was recently suggested that in VSM cells and cardiac myocytes cGMP signaling may be spatially segregated and that this functional compartmentalization may be the cause of the unique actions of ANP and NO (19–23). The goal of this study was to develop previously undescribed non-FRET biosensors suitable to monitor the temporal changes of $[cGMP]_i$ in response to low-nanomolar NO or ANP, and to investigate the spatial patterning of $[cGMP]_i$, using real-time, confocal imaging techniques.

The concept of non-FRET based biosensors, containing a single GFP-based fluorescence unit was first described by Tsien and colleagues with the development of Ca^{2+}-sensitive "camgaroos," by placing calmodulin at an insertion-permissive site within the β sheets of GFP (24). Subsequently, circularly permutated EGFP (cpEGFP) advanced non-FRET based biosensors even further and gave rise to the development of "GCaMP"-type Ca^{2+} indicators, in which the Ca^{2+}-dependent interaction between calmodulin and its specific binding protein M13 was directly translated into conformational changes and an increase in fluorescence intensity of the single fluorescent molecule cpEGFP (25, 26). We adopted this concept of non-FRET biosensors to design cGMP indicators, called FlincGs (fluorescent indicators of cGMP). FlincG indicators are composed of cpEGFP, N-terminally fused to regulatory domain fragments of PKG. The overall favorable kinetic and spectroscopic characteristics of this single emission detection system permits the direct examination of local cGMP dynamics in response to low-nanomolar NO or ANP in VSM cells in real-time.

Results and Discussion

Bioengineering FlincG Biosensors from Type I PKG. FlincGs are composed of two in-tandem, PKG derived cGMP binding sites fused to the N terminus of cpEGFP (Fig. 1*A*). In contrast to GCaMP-type calcium indicators (25), FlincGs do not require intramolecular protein–protein interactions between separate domains. Instead, dose-dependent binding of cGMP to both receptor domains was sufficient to increase fluorescence intensity in cpEGFP (Fig. 1*C Inset*). Previous studies using hydrodynamic and small-angle x-ray scattering techniques support our findings that cGMP binding to the regulatory domain of PKG I induces substantial conformational changes (27–29). α-FlincG was developed by attaching the entire regulatory domain of PKG I α (residues 1–356) to cpEGFP (Fig. 1*B*). cGMP increased fluorescence intensity of this construct by up to 1.5-fold, with an apparent K_D of 35 nM (Fig. 1*C*) and with an ≈1,100-fold selectivity for cGMP over cAMP (Table 1).

To increase the dynamic range of $[cGMP]_i$ detection, we took advantage of the fact that the activation constants of PKG I α

Author contributions: L.W.M.N. and W.R.D. designed research; L.W.M.N. performed research; J.L. and A.D.B. contributed new reagents/analytic tools; L.W.M.N. and J.L. analyzed data; and L.W.M.N., M.T.N., and W.R.D. wrote the paper.

The authors declare no conflict of interest.

*To whom correspondence should be addressed at: University of Vermont, Department of Pharmacology, Health Science Research Facility 330, 149 Beaumont Avenue, Burlington, VT 05405-0075. E-mail: wdostman@uvm.edu.

This article contains supporting information online at www.pnas.org/cgi/content/full/0710387105/DC1.

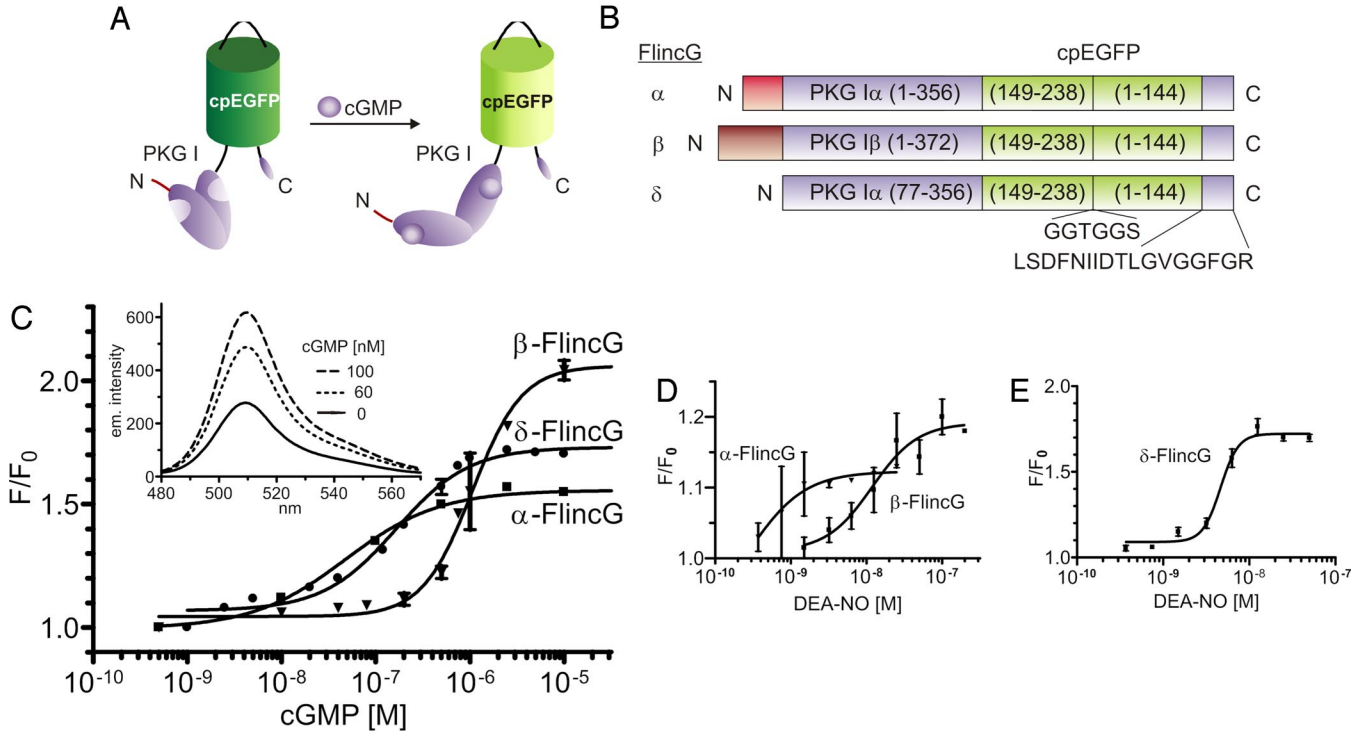

Fig. 1. Characterization of FlincG biosensors as recombinant proteins and in VSM cells. (*A*) Schematic architecture: fusion of regulatory fragments of PKG I to cpEGFP induces cGMP dependent changes in fluorescence emission intensity. (*B*) Domain structure: α-, β- and δ-FlincG use regulatory fragments of PKG I α and PKG I β. (*C*) cGMP dose–response curves for α-, β- and δ-FlincG (Table 1). (*Inset*) cGMP dose-dependent increase in fluorescence intensity shown for α-FlincG. (*D* and *E*) NO-titration of α- and β-FlincG (*D*) and δ-FlincG (*E*) in single VSM cells using epi-fluorescence microscopy (see Table 2).

and I β shift from 75 nM to ≈1.0 to 1.8 μM (30–32). PKG I α and I β are genetic splice-variants and consist of different N-termini, but are virtually identical within their cGMP binding and catalytic domains (30). Thus, we developed β-FlincG, by connecting the regulatory domain of PKG I β to the N terminus of cpEGFP (Fig. 1*B*). As predicted, this FlincG variant demonstrated a shifted cGMP binding constant of 1.1 μM (Fig. 1*C* and Table 1), indicating the significance of the N terminus for modulating cGMP binding affinities. Interestingly, removal of the entire N-terminal domain (Δ1–77) of PKG I α resulted in δ-FlincG, which exhibited an apparent K_D of 170 nM. This result is in accordance to an analogous PKG I α deletion fragment, Δ1–77/352–670 for which a similar cGMP binding constant (K_D = 218 nM) has been reported (33). This finding further supports the concept that the N-terminal domain of PKG, not the catalytic domain, primarily modulates cGMP binding affinities of the FlincG indicators. Interestingly, the C terminus of FlincGs did not affect fluorescence intensity changes. Neither the linker sequence shown in Fig. 1*B*, which was the product of a randomized cloning approach, nor attachment of the PKG catalytic domain, or complete removal of any C-terminal appendage had any effect on overall fluorescence intensity changes (data not shown).

Under cell-free conditions, α- and β-FlincG exhibited maximal 1.5 and 2.1-fold intensity changes, respectively (Fig. 1*C* and Table 1). When expressed in VSM cells, the maximal fluorescence increases of α- and β-FlincG were reduced to ≈1.2-fold, although these indicators retained high NO-sensitivity ($EC_{50,DEA-NO}$ = 0.3 and 12 nM, respectively) (Table 2 and Fig. 1*D*). Both biosensors contain their respective N-terminal PKG dimerization sequences, which may give rise to interactions with endogenous PKG and thus decreases their observed maximal intensity changes (Fig. 1*D* and Table 2). In support of this idea, coimmunoprecipitation experiments demonstrated formation of mixed dimers between wild-type PKG and α-, or β-FlincG (supporting information (SI) Fig. 6). However, δ-FlincG did not display any interaction with wild-type PKG, because it lacks the N-terminal dimerization domain (SI Fig. 6). Therefore, we did not observe a reduction of maximal fluorescence intensity when comparing purified δ-FlincG to indicator expressed in intact VSM cells (Figs. 1 *C* and E), whilst retaining high NO sensitivity ($EC_{50,DEA-NO}$ = 4 nM; Fig. 1*E*). This indicator was also highly selective for cGMP over cAMP (>280-fold, Table 1).

Table 1. cGMP and cAMP selectivity of recombinant FlincG biosensors

FlincG isoform	$(F/F_0)_{max}$	$K_{D,cGMP}$, μM	$K_{D,cAMP}$, μM	cGMP/cAMP
Alpha*	1.55 ± 0.05 [4]	0.035 ± 0.010 [4]	40 ± 8 [3]	1,140
Beta*	2.05 ± 0.03 [5]	1.100 ± 0.050 [5]	31 ± 10 [4]	30
Delta*	1.75 ± 0.03 [5]	0.170 ± 0.020 [5]	48 ± 10 [4]	280
Delta†	3.50 ± 0.06 [4]	0.488 ± 0.004 [4]	48 ± 10 [4]	100

*Single excitation at 480 nm, emission at 510 nm (Fig. 1*C*).
†Ratiometric excitation at 410 and 480 nm, emission at 510 nm (Fig. 2*D*). The values represent the mean ± SEM of *n* numbers of experiments (shown in brackets).

Table 2. NO-titration and calibration of FlincG biosensors in VSM cells

FlincG isoform	EC_{50}, DEA-NO, nM	EC_{50}, PROLI-NO, nM	$(F/F_0)_{max}$	EC_{50}, cGMP*, nM
Alpha	0.3 ± 0.2 [6]	—	1.12 ± 0.08	—
Beta	12 ± 0.4 [6]	—	1.19 ± 0.06	—
Delta	4 ± 0.5 [8]	16 ± 2 [6]	1.75 ± 0.03	150 ± 12 [4]

*Calibration for cGMP in β-escin permeabilized VSM cells. The values represent the mean ± SEM of *n* numbers of experiments (shown in brackets).

Recently published FRET cGMP-sensors by Russwurm *et al.* (11) display a comparable maximal FRET ratio change of 75% for recombinant protein. In living cells however, all FRET-indicators published so far, exhibit a significant decrease in maximal FRET ratio change, ranging from 35% to 45% (9–12). In contrast, FlincG cGMP biosensors have been designed to minimize interactions with endogenous proteins and to maintain maximal fluorescence intensity changes in living cells while retaining nanomolar NO sensitivity. Because δ-FlincG exhibits all these favorable characteristics in living cells, we selected δ-FlincG as indicator suitable for studying intracellular cGMP dynamics.

Kinetic, Spectral Analysis and Environmental Stability of δ-FlincG. A more refined spectral analysis revealed that in addition to the 491 excitation maximum, δ-FlincG displayed a second, blue-shifted excitation peak at 410 nm (Fig. 2*A*). Furthermore, these excitation maxima at 410 and 491 nm respond differentially in response to 1 μM cGMP. It should be noted, that all FlincG indicators possessed this secondary 410 nm excitation maximum (data not shown), but only for δ-FlincG cGMP decreased the emission intensity at 410 nm 0.5-fold, with a corresponding emission maximum at 507 nm (Fig. 2*B*). In addition, excitation at 480 nm yielded an emission maximum at 511 nm (Fig. 2*C*) with an overall 1.75-fold fluorescence intensity increase. Thus, our results are in contrast to the excitation emission spectra of EGFP and previous cpEGFP based indicators, such as camgaroos and GCaMPs, which display only one excitation maximum at 489 nm (24, 25, 34).

Based on its dual excitation spectrum, δ-FlincG offers several

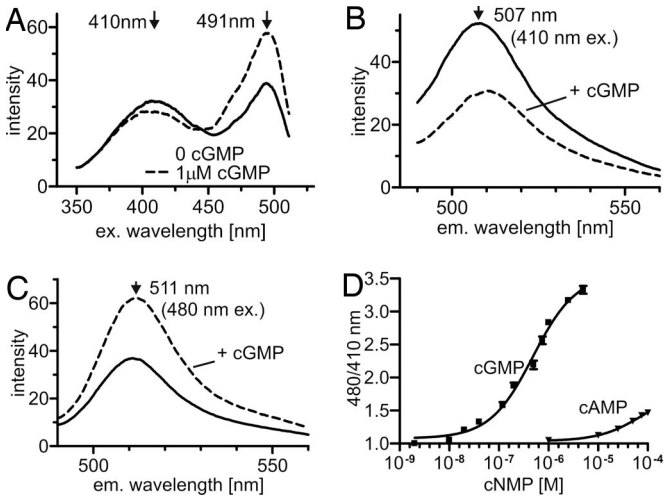

Fig. 2. Spectral analysis of δ-FlincG. (*A*) Excitation spectrum of δ-FlincG in presence and absence of 1 μM cGMP detected at 510 nm. (*B* and *C*) Emission spectra excited at 410 (*B*) and 480 (*C*) nm in the presence and absence of 1 μM cGMP. (*D*) Ratiometric (480/410 nm) dose–response curves for cGMP and cAMP detected at 510 nm.

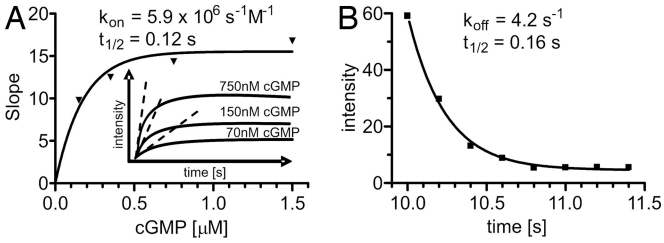

Fig. 3. cGMP binding kinetics of δ-FlincG. (*A*) cGMP association kinetics using stopped-flow fluorometry. (*Inset*) Slopes represent the initial association velocities at different cGMP concentrations. (*B*) cGMP dissociation kinetics using a dilution protocol (see *Materials and Methods*). Intensity changes were detected by using a fluo-spectrophotometer.

technical alternatives to previous FRET-based cGMP imaging techniques. First, the two excitation wavelengths may be combined and analyzed ratiometrically (480/410 nm excitation), similar to the Ca^{2+} indicator Fura (35). As a result, the overall ratio change increased up to 3.5-fold *in vitro*, and the overall apparent $K_{D,cGMP}$ was 488 nM, with ≈100-fold selectivity for cGMP over cAMP (Fig. 2*D* and Table 1). Second, a single wavelength excitation system could be used by employing a 410/510 nm excitation/emission detection profile. However, for the initial experiments with δ-FlincG, the single wavelength approach (480/510 nm excitation/emission) was used, because it is faster, has decreased risk of photo-bleaching, superior cGMP/cAMP selectivity, and an advantageous apparent cGMP binding constant of 170 nM (Fig. 1*C* and Table 1). Nonetheless, in future studies, the ratiometric approach (Fig. 2*D*) would present a number of significant inherent advantages, including the determination of $[cGMP]_i$.

To examine further δ-FlincG's utility as a $[cGMP]_i$-biosensor, we investigated its environmental stability under varying pH conditions (SI Fig. 7). Previously reported cpGFP based biosensors, such as camgaroos and GCaMPs, have displayed significant pH sensitivity under physiological conditions with pK_a values of 8.9 and 7.1, respectively (24, 25). Elaborate mutational approaches have been undertaken to reduce the environmental sensitivity of GFP and GFP-based variants. So far, only Citrine, a yellow fluorescent protein (YFP)-based mutant, has been reported with superior chloride and pH stability (pK_a 5.7) compared with previous YFPs (34). In comparison, our results indicate that δ-FlincG did not require mutational optimization to accomplish resistance to small changes in pH under physiological conditions (pK_a 6.1).

An important requirement for a biosensor is to have fast kinetics so that intracellular temporal and spatial changes can be accurately monitored. Stopped-flow experiments revealed a fast rate of cGMP association ($k_{on} = 5.9 \times 10^6\ s^{-1}{\cdot}M^{-1}$; $t_{1/2} = 0.12$ s) (Fig. 3*A* and Table 3). The dissociation constant determined by protein dilution was equally rapid ($k_{off} = 4.2\ s^{-1}$; $t_{1/2} = 0.16$ s) (Fig. 3*B* and Table 3). These rate constants ensure that the rate limiting step for detecting $[cGMP]_i$ does not occur at the level of cGMP association to or dissociation from the biosensor. Equally advantageous, δ-FlincG should not act as a sink for $[cGMP]_i$, because its cGMP binding constant (170 nM) is not significantly different from its major endogenous receptors PKG I α and PDE

Table 3. cGMP association and dissociation kinetics

FlincG isoform	k_{on}, $s^{-1}M^{-1}$	$t_{1/2}$*, s	k_{off}, s^{-1}	$t_{1/2}$†, s
Delta	5.9×10^6 [4]	0.12 [4]	4.2 [3]	0.16 [3]

*$t_{1/2}$ cGMP association.
†$t_{1/2}$ cGMP dissociation. The values represent the mean ± SEM of *n* numbers of experiments (shown in brackets).

PHARMACOLOGY

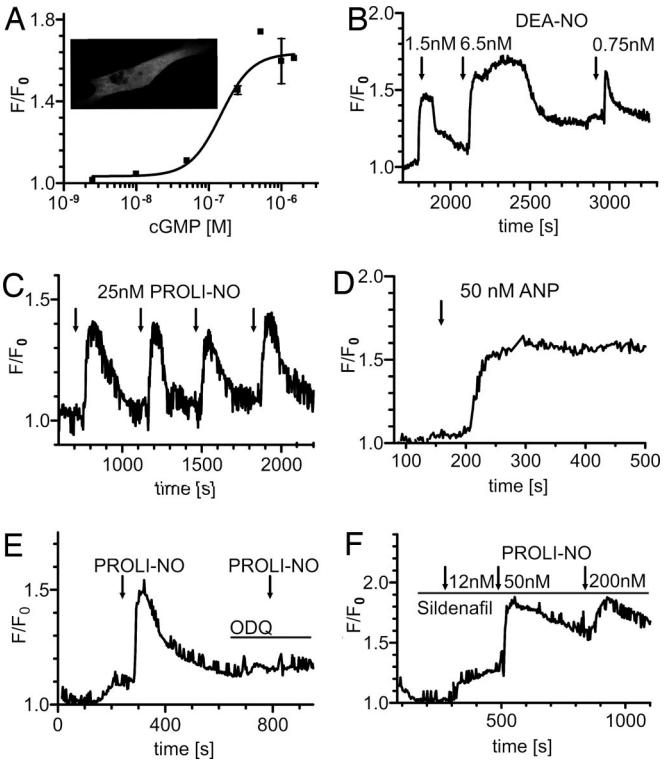

Fig. 4. Temporal dynamics of cGMP in VSM cells. (*A*) Calibration of δ-FlincG. Adenovirus-transfected VSM cells (*Inset*) were permeabilized with β-escin and exposed to increasing cGMP concentrations (25 nM to 2 μM). (*B* and *C*) Temporal cGMP dynamics in VSM cells were analyzed upon addition of 0.75–6.5 nM DEA-NO (*B*), 25 nM PROLI-NO (*C*), and 50 nM ANP (*D*) using epi-fluorescence microscopy. (*E* and *F*) Effects of ODQ and Sildenafil on δ-FlincG-transfected VSM cells. Cells were exposed repeatedly to 50 nM PROLI-NO in presence and absence of 10 μM ODQ (*E*) and to 12–200 nM PROLI-NO in presence of 50 μM Sildenafil (*F*). For each experimental series, *n* numbers are 4–10.

5 in vascular smooth muscle (30, 36). Superior spectral characteristics, environmental stability and fast association/dissociation kinetics should enable δ-FlincG to capture the rapid rise and fall of $[cGMP]_i$ in living VSM cells.

Intracellular Properties of δ-FlincG in Vascular Smooth Muscle Cells. Recently, we reported that primary, unpassaged VSM cells from rat aorta retain the expression of key cGMP-signaling enzymes, such as PKG I, sGC and PDE5 (12). Transfection of VSM cells with δ-FlincG adenovirus resulted in an even cytosolic distribution and nuclear exclusion of the indicator, with a 90% efficiency (Fig. 4*A Inset*). To determine the apparent affinity of intracellular δ-FlincG for cGMP, VSM cells were permeabilized with β-escin and the cells were exposed to different levels of cGMP in Ca^{2+}-free imaging buffer. Half-maximal fluorescence increases occurred at 150 nM cGMP (Fig. 4*A*), similar to the value obtained for the purified biosensor (170 nM; Fig. 1*C*). With this approach, the level of intracellular cGMP can be estimated from the fractional change in fluorescence.

An important criterion for intracellular cGMP sensors is that they exhibit appropriately high sensitivity to NO, as previously reported for sGC (half-maximal NO: 1.7 nM for the purified enzyme, 11 nM for intact platelets, 10 nM for cerebellar cells) (17, 18). DEA-NO and PROLI-NO were used as NO-donors due to their overall favorable fast chemistry of NO-release (see *Materials and Methods*). DEA-NO (0.75–6.50 nM) induced concentration-dependent, transient increases in $[cGMP]_i$, corresponding to 10 nM to 1 μM (Fig. 4 *A* and B). The corresponding half activation

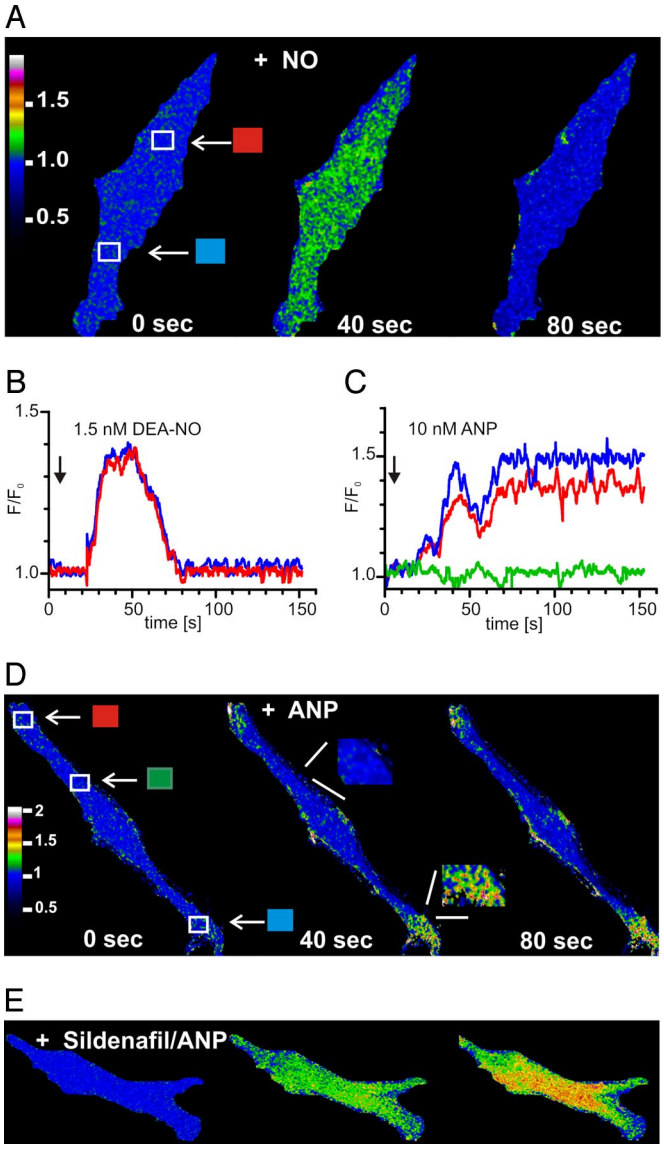

Fig. 5. Spatial analysis of the NO and ANP pools of cGMP in δ-FlincG transfected VSM cells. $[cGMP]_i$ in response to 1.5 nM DEA-NO (*A* and *B*) and 10 nM ANP (*C* and *D*) using confocal microscopy. Regions of interest and their corresponding intensity traces are indicated with arrows and corresponding color boxes. Acquisition speed = 5 frames per s; exposure time = 64 ms. (*E*) Application of 10 nM ANP after preincubation with 100 μM Sildenafil. For each experimental series, *n* numbers are 4–6.

constant ($EC_{50,DEA-NO}$) was 4 nM (Fig. 1*E* and Table 2). Similarly, transient and highly reproducible $[cGMP]_i$ changes were observed with 25 nM PROLI-NO ($EC_{50,PROLI-NO}$ = 16 nM; Table 2; Fig. 4*C*). In contrast to NO-stimulated sGC, activation of the plasma membrane-associated guanylyl cyclase pGC-A using atrial natriuretic peptide (ANP) resulted in sustained levels of $[cGMP]_i$ (Fig. 4*D*), as demonstrated previously in VSM cells using radio-immunoassays (37–39). These results promote δ-FlincG as exceptional biosensor for physiological (low-nanomolar) NO- and ANP-induced cGMP dynamics in VSM cells.

NO-induced elevation of $[cGMP]_i$ requires activation of sGC. ODQ (10 μM), a specific inhibitor of sGC activation (40–42), prevented the PROLI-NO (50 nM) induced increase of cGMP (Fig. 4*E*), indicating that the observed rise in $[cGMP]_i$ is indeed due to NO-induced activation of sGC. The $[cGMP]_i$ also depends on its hydrolysis by PDE-5. Sildenafil, a PDE-5-specific inhibitor

(43, 44), greatly slowed the decay in $[cGMP]_i$ in response to PROLI-NO (12 to 200 nM), supporting the concept of a dynamic interplay between sGC production and PDE-5 mediated hydrolysis of cGMP (Fig. 4*F*).

Spatial and Temporal Dynamics of NO- and ANP-Induced cGMP Signaling in δ-FlincG-Transfected Vascular Smooth Muscle Cells. Our current understanding of the intracellular distribution of cGMP derives from the fact that the predominant soluble guanylyl cyclase isoform sGC-$\alpha_1\beta_1$ is largely cytosolic; therefore, $[cGMP]_i$ should be cytosolic as well (6). The natriuretic peptides ANP, BNP and CNP, in contrast, specifically activate plasma membrane-associated guanylyl cyclases pGC-A and pGC-B and thus, may give rise to a distinct spatial pattern of $[cGMP]_i$ (22, 23). However, the spatial distribution of $[cGMP]_i$ in response to NO and ANP has never been studied by the means of high resolution confocal imaging techniques. FlincG-indicators should permit the measurement of cGMP patterns in living cells.

A physiological dose of 1.5 nM NO induced a global, but transient, elevation in $[cGMP]_i$ (Fig. 5 *A* and B; SI Movie 1), similar to measurements conducted with lower resolution, epi-fluorescence microscopy (Fig. 4 *B* and *C*). The membrane-permeant cGMP analog (8-Br-cGMP, 50 μM) was applied to VSM cells and a uniform increase in fluorescence was observed (SI Movie 2), indicating homogenous expression of δ-FlincG in VSM cells. Forskolin (100 nM), which specifically activates the cAMP signaling pathway, had no effect on fluorescence intensity (SI Movie 3), consistent with δ-FlincG selectivity for cGMP over cAMP.

In contrast to the transient NO-evoked $[cGMP]_i$ patterns, application of ANP (10 nM) induced sustained synthesis of at least 1 μM $[cGMP]_i$ (Fig. 5 *C* and *D*). This finding is in agreement with our results shown in Fig. 4*D*, although different imaging techniques (epi- versus confocal microscopy) give rise to variations in the onset of ANP response (mean lag time: 25 ± 4 s, Fig. 5*C*; 45 ± 10 s, Fig. 4*D*). ANP induced local, spatially segregated patterns of $[cGMP]_i$ at the plasma membrane of single VSM cells (Fig. 5*D* and SI Movie 4). To address spatial patterning due to uneven indicator expression and cell movement, which may present potential problems in single wavelength intensity measurements, we analyzed three-dimensional surface plots (SI Fig. 8) indicating uniform cellular distribution of δ-FlincG (from Fig. 5 *A* and *D*). SI Fig. 9 verifies that the cell morphology does not change over time after NO or ANP application and that the cells do not move.

Spatially confined cGMP signaling may be a combination of both local cGMP synthesis and local degradation at the membrane. Recently, compartmentalized $[cGMP]_i$ was reported in cardiac myocytes through specific activation of pGC by natriuretic peptides (15, 19, 21). These studies also suggested that cGMP-specific PDEs maintain these local patterns of $[cGMP]_i$ elicited through pGC. Our results indicate that ANP (10 nM) induced cGMP synthesis is sustained and spatially confined in VSM cells (Fig. 5 *C* and *D*). This spatial localization in response to ANP was abolished, when VSM cells were preincubated with the PDE-5 inhibitor, sildenafil (Fig. 5*E*). Instead, a global increase in $[cGMP]_i$ was observed, indicating that degradation of cGMP by PDE-5 prevents the cell's interior from experiencing an elevation of cGMP. These ANP-produced submembrane cGMP elevations suggest local targeting of submembrane targets such as the calcium-sensitive (BK) channel and SERCA-regulatory protein, phospholamban (45, 46).

In conclusion, FlincG represents a previously undescribed generation of cGMP biosensors that excels in monitoring $[cGMP]_i$ in response to physiological (low-nanomolar) NO concentrations. FlincG should ultimately be suitable for development of tissue-specific generation of transgenic mice with endogenous cGMP indicators, as has been done recently for calcium sensing with GCaMP (26, 47). The ratiometric possibilities of FlincG should enhance its versatility. FlincG revealed the differential role of PDE-5 in the modulation of global cGMP in response to NO donors, and the spatial spread of cGMP away from the cell membrane in response to ANP. FlincG holds the promise of unraveling the complex interplay between cGMP and calcium signaling near the cell membrane.

Materials and Methods

Fluorescence Measurements in Cultured Vascular Smooth Muscle Cells (P0). VSM cells were harvested from rat aortic tissue and cultured as described in ref. 12. For transfection, 100 μl of adenovirus (10^7 to 10^9 per ml titer) were applied to 50% confluent VSM cells (P0) and incubated 24 to 48 h at 37°C, 5% CO_2 until a 90% transfection efficiency in VSM cells was achieved. Epi-fluorescence imaging was performed by incubating cells in imaging buffer [10 mM TES (pH 7.4), 1 g/liter D-glucose, Hank's balanced salt solution (HBSS; Mediatech, Inc., Herndon, VA)] at 37°C using a Delta T4 open culture system (Bioptechs, Butler, PA). A Nikon Diaphot 200 microscope outfitted with a Nikon ×40/1.30 oil objective, a cooled charge-coupled device camera (ORCA ER; Hamamatsu, Japan), and a mercury-halide lamp (X-CITE 120; EXFO Photonics, Toronto) were used to image individual cells with 3 seconds acquisitions. Imaging of FlincG indicators was controlled by Metafluor 6.2 software (Universal Imaging, Media, PA) using a D480/20m excitation filter, 505drxr dichroic mirror and D535/30m emission. For confocal imaging, P0 VSM cells were imaged by using a spinning disk confocal system (Andor) outfitted on a Nikon E600SN microscope with a ×60 water dipping objective (N.A. 1.0), and iXon ENCCD DVB camera with 5 frames per s acquisition speed and 64-ms exposure time exciting with a solid state laser at 488 nm, and collecting the emission at 510 nm. Data analysis was performed with custom written software developed by Adrian Bonev. For confocal microscopy, cGMP responses were investigated upon local application (5 to 50 μl) and subsequent diffusion of DEA/NONOate (Calbiochem), PROLI/NONOate (Cayman Chemicals), ANP (Sigma), Sildenafil (Pfizer), ODQ (Sigma), 8-Br-cGMP (BioLog), and Forskolin (Sigma). Approximately 75% of the data collected were rejected because of cell movement and morphology changes during the course of the experiments. For epi-fluorescence microscopy, chemicals were distributed evenly by mixing with imaging buffer. Calibration of adenoviral transfected VSM cells was performed in Hepes-buffered, Ca^{2+}-free PSS pH 7.4. VSM cells were permeabilized with 20 μM β-escin, exposed to increasing cGMP concentrations (0–2 μM) and analyzed by using the epi-fluorescence microscope facility. For NO-titration, δ-FlincG transfected VSM cells were exposed to 0.4–500 nM DEA-NO ($t_{1/2}$ = 2.4 min at 37°C, pH 7.4), or to 1.5 nM to 2 μM PROLI-NO ($t_{1/2}$ = 1.8 s at 37°C, pH 7.4). Data were analyzed by using the Metafluor software and dose-response curves were calculated with GraphPadPrism.

Further methods are provided in *SI Materials and Methods*.

ACKNOWLEDGMENTS. We thank Dr. Alan Howe (University of Vermont, Burlington, VT) for providing anti-GFP antibodies and Dr. Christopher Berger (University of Vermont, Burlington, VT) for assistance with the stopped-flow equipment. This work was supported by National Institutes of Health (NIH) Grant HL68891 and National Science Foundation Grant MCB-9983097 (to W.R.D.), by NIH Grants HL44455, DK53832, DK65947, and HL77378 (to M.T.N.), by the Canadian Institutes for Health Research, by Fonds de Recherche en Santé du Québec, and by the Totman Trust for Medical Research.

1. Conti M, Beavo J (2007) Biochemistry and physiology of cyclic nucleotide phosphodiesterases: Essential components in cyclic nucleotide signaling. *Annu Rev Biochem* 76:481–511.
2. Francis SH, Blount MA, Zoraghi R, Corbin JD (2005) Molecular properties of mammalian proteins that interact with cGMP: Protein kinases, cation channels, phosphodiesterases, and multi-drug anion transporters. *Front Biosci* 10:2097–2117.
3. Hofmann F, Biel M, Kaupp UB (2005) International Union of Pharmacology. LI. Nomenclature and structure-function relationships of cyclic nucleotide-regulated channels. *Pharmacol Rev* 57:455–462.
4. Hofmann F (2005) The biology of cyclic GMP-dependent protein kinases. *J Biol Chem* 280:1–4.
5. Kuhn M (2005) Cardiac and intestinal natriuretic peptides: Insights from genetically modified mice. *Peptides* 26:1078–1085.
6. Mullershausen F, Koesling D, Friebe A (2005) NO-sensitive guanylyl cyclase and NO-induced feedback inhibition in cGMP signaling. *Front Biosci* 10:1269–1278.
7. Garthwaite J (2005) Dynamics of cellular NO-cGMP signaling. *Front Biosci* 10:1868–1880.
8. Cary SP, Winger JA, Derbyshire ER, Marletta MA (2006) Nitric oxide signaling: No longer simply on or off. *Trends Biochem Sci* 31:231–239.
9. Honda A, Adams SR, Sawyer CL, Lev-Ram V, Tsien RY, Dostmann WR (2001) Spatiotemporal dynamics of guanosine 3′,5′-cyclic monophosphate revealed by a genetically encoded, fluorescent indicator. *Proc Natl Acad Sci USA* 98:2437–2442.

10. Nikolaev VO, Gambaryan S, Lohse MJ (2006) Fluorescent sensors for rapid monitoring of intracellular cGMP. *Nat Methods* 3:23–25.
11. Russwurm M, *et al*. (2007) Design of fluorescence resonance energy transfer (FRET)-based cGMP indicators: A systematic approach. *Biochem J* 407:69–77.
12. Cawley SM, Sawyer CL, Brunelle KF, van der Vliet A, Dostmann WR (2007) Nitric oxide-evoked transient kinetics of cyclic GMP in vascular smooth muscle cells. *Cell Signal* 19:1023–1033.
13. Honda A, Sawyer CL, Cawley SM, Dostmann WR (2005) Cygnets: *In vivo* characterization of novel cGMP indicators and *in vivo* imaging of intracellular cGMP. *Methods Mol Biol* 307:27–43.
14. Takimoto E, *et al*. (2005) cGMP catabolism by phosphodiesterase 5A regulates cardiac adrenergic stimulation by NOS3-dependent mechanism. *Circ Res* 96:100–109.
15. Mongillo M, *et al*. (2006) Compartmentalized phosphodiesterase-2 activity blunts beta-adrenergic cardiac inotropy via an NO/cGMP-dependent pathway. *Circ Res* 98:226–234.
16. Honda A, Moosmeier MA, Dostmann WR (2005) Membrane-permeable cygnets: Rapid cellular internalization of fluorescent cGMP-indicators. *Front Biosci* 10:1290–1301.
17. Mo E, Amin H, Bianco IH, Garthwaite J (2004) Kinetics of a cellular nitric oxide/cGMP/phosphodiesterase-5 pathway. *J Biol Chem* 279:26149–26158.
18. Roy B, Garthwaite J (2006) Nitric oxide activation of guanylyl cyclase in cells revisited. *Proc Natl Acad Sci USA* 103:12185–12190.
19. Castro LR, Verde I, Cooper DM, Fischmeister R (2006) Cyclic guanosine monophosphate compartmentation in rat cardiac myocytes. *Circulation* 113:2221–2228.
20. Piggott LA, *et al*. (2006) Natriuretic peptides and nitric oxide stimulate cGMP synthesis in different cellular compartments. *J Gen Physiol* 128:3–14.
21. Takimoto E, *et al*. (2007) Compartmentalization of cardiac beta-adrenergic inotropy modulation by phosphodiesterase type 5. *Circulation* 115:2159–2167.
22. Fischmeister R, *et al*. (2006) Compartmentation of cyclic nucleotide signaling in the heart: The role of cyclic nucleotide phosphodiesterases. *Circ Res* 99:816–828.
23. Kass DA, Takimoto E, Nagayama T, Champion HC (2007) Phosphodiesterase regulation of nitric oxide signaling. *Cardiovasc Res* 75:303–314.
24. Baird GS, Zacharias DA, Tsien RY (1999) Circular permutation and receptor insertion within green fluorescent proteins. *Proc Natl Acad Sci USA* 96:11241–11246.
25. Nakai J, Ohkura M, Imoto K (2001) A high signal-to-noise Ca(2+) probe composed of a single green fluorescent protein. *Nat Biotechnol* 19:137–141.
26. Tallini YN, *et al*. (2006) Imaging cellular signals in the heart *in vivo*: Cardiac expression of the high-signal Ca^{2+} indicator GCaMP2. *Proc Natl Acad Sci USA* 103:4753–4758.
27. Richie-Jannetta R, Busch JL, Higgins KA, Corbin JD, Francis SH (2006) Isolated regulatory domains of cGMP-dependent protein kinase I alpha and I beta retain dimerization and native cGMP-binding properties and undergo isoform-specific conformational changes. *J Biol Chem* 281:6977–6984.
28. Wall ME, *et al*. (2003) Mechanisms associated with cGMP binding and activation of cGMP-dependent protein kinase. *Proc Natl Acad Sci USA* 100:2380–2385.
29. Zhao J, *et al*. (1997) Progressive cyclic nucleotide-induced conformational changes in the cGMP-dependent protein kinase studied by small angle x-ray scattering in solution. *J Biol Chem* 272:31929–31936.
30. Ruth P, *et al*. (1991) The activation of expressed cGMP-dependent protein kinase isozymes I alpha and I beta is determined by the different amino-termini. *Eur J Biochem* 202:1339–1344.
31. Ruth P, *et al*. (1997) Identification of the amino acid sequences responsible for high affinity activation of cGMP kinase I alpha. *J Biol Chem* 272:10522–10528.
32. Wolfe L, Corbin JD, Francis SH (1989) Characterization of a novel isozyme of cGMP-dependent protein kinase from bovine aorta. *J Biol Chem* 264:7734–7741.
33. Dostmann WR, Koep N, Endres R (1996) The catalytic domain of the cGMP-dependent protein kinase I alpha modulates the cGMP-binding characteristics of its regulatory domain. *FEBS Lett* 398:206–210.
34. Griesbeck O, Baird GS, Campbell RE, Zacharias DA, Tsien RY (2001) Reducing the environmental sensitivity of yellow fluorescent protein: Mechanism and applications. *J Biol Chem* 276:29188–29194.
35. Grynkiewicz G, Poenie M, Tsien RY (1985) A new generation of Ca^{2+} indicators with greatly improved fluorescence properties. *J Biol Chem* 260:3440–3450.
36. Zoraghi R, Bessay EP, Corbin JD, Francis SH (2005) Structural and functional features in human PDE5A1 regulatory domain that provide for allosteric cGMP binding, dimerization, and regulation. *J Biol Chem* 280:12051–12063.
37. Winquist RJ, Faison EP, Waldman SA, Schwartz K, Murad F, Rapoport RM (1984) Atrial natriuretic factor elicits an endothelium-independent relaxation and activates particulate guanylate cyclase in vascular smooth muscle. *Proc Natl Acad Sci USA* 81:7661–7664.
38. Leitman DC, *et al*. (1988) Atrial natriuretic peptide binding, cross-linking, and stimulation of cyclic GMP accumulation and particulate guanylate cyclase activity in cultured cells. *J Biol Chem* 263:3720–3728.
39. Hamet P, Pang SC, Tremblay J (1989) Atrial natriuretic factor-induced egression of cyclic guanosine 3′:5′-monophosphate in cultured vascular smooth muscle and endothelial cells. *J Biol Chem* 264:12364–12369.
40. Garthwaite J, *et al*. (1995) Potent and selective inhibition of nitric oxide-sensitive guanylyl cyclase by 1H-[1,2,4]oxadiazolo[4,3-a]quinoxalin-1-one. *Mol Pharmacol* 48:184–188.
41. Brunner F, Stessel H, Kukovetz WR (1995) Novel guanylyl cyclase inhibitor, ODQ reveals role of nitric oxide, but not of cyclic GMP in endothelin-1 secretion. *FEBS Lett* 376:262–266.
42. Schrammel A, Behrends S, Schmidt K, Koesling D, Mayer B (1996) Characterization of 1H-[1,2,4]oxadiazolo[4,3-a]quinoxalin-1-one as a heme-site inhibitor of nitric oxide-sensitive guanylyl cyclase. *Mol Pharmacol* 50:1–5.
43. Turko IV, Ballard SA, Francis SH, Corbin JD (1999) Inhibition of cyclic GMP-binding cyclic GMP-specific phosphodiesterase (Type 5) by sildenafil and related compounds. *Mol Pharmacol* 56:124–130.
44. Corbin JD, *et al*. (2003) [3H]Sildenafil binding to phosphodiesterase-5 is specific, kinetically heterogeneous, and stimulated by cGMP. *Mol Pharmacol* 63:1364–1372.
45. Robertson BE, Schubert R, Hescheler J, Nelson MT (1993) cGMP-dependent protein kinase activates Ca-activated K channels in cerebral artery smooth muscle cells. *Am J Physiol* 265:C299–303.
46. Porter VA, *et al*. (1998) Frequency modulation of Ca^{2+} sparks is involved in regulation of arterial diameter by cyclic nucleotides. *Am J Physiol* 274:C1346–C1355.
47. Ji G, *et al*. (2004) Ca^{2+}-sensing transgenic mice: Postsynaptic signaling in smooth muscle. *J Biol Chem* 279:21461–21468.